Physics Letters B 761 (2016) 310–317

Contents lists available at ScienceDirect

Physics Letters B

www.elsevier.com/locate/physletb

Has a Higgs-flavon with a 750 GeV mass been detected at the LHC13?

A. Bolaños [a], J.L. Diaz-Cruz [b], G. Hernández-Tomé [b], G. Tavares-Velasco [b,*]

[a] Facultad de Física, Universidad Veracruzana, 91000, Xalapa, Veracruz, Mexico
[b] Facultad de Ciencias Físico-Matemáticas, Benemérita Universidad Autónoma de Puebla, C.P. 72570, Puebla, Puebla, Mexico

ARTICLE INFO

Article history:
Received 30 April 2016
Received in revised form 11 August 2016
Accepted 12 August 2016
Available online 18 August 2016
Editor: M. Cvetič

ABSTRACT

Higgs-flavon fields appear as a part of the Froggatt–Nielsen (FN) mechanism, which attempts to explain the hierarchy of Yukawa couplings. We explore the possibility that the 750 GeV diphoton resonance recently reported at the LHC13 could be identified with a low-scale Higgs-flavon field H_F and find the region of the parameter space consistent with CMS and ATLAS data. It is found that the extra vector-like fermions of the ultraviolet completion of the FN mechanism are necessary in order to reproduce the observed signal. We consider a standard model (SM) extension that contains two Higgs doublets (a standard one and an inert one) and one complex FN singlet. The inert doublet includes a stable neutral boson, which provides a viable dark matter candidate, while the mixing of the standard doublet and the FN singlet induces flavor violation in the Higgs sector at the tree-level. Constraints on the parameters of the model are derived from the LHC Higgs data, which include the search for the lepton flavor violating decay of the SM Higgs boson $h \to \bar{\mu}\tau$. It is also found that in some region of the parameter space the model may give rise to a large branching ratio for the $H_F \to hh$ decay, of the order of 0.1, which could be searched for at the LHC.

1. Introduction

Preliminary results of the LHC Run at 13 TeV showed surprising hints of a resonance in the diphoton channel with invariant mass of 750 GeV [1,2], which could represent a signal of physics beyond the standard model (SM). The ATLAS collaboration collected 3.2 fb^{-1} of data and reports a signal with significance of 3.6 σ (local), which becomes 2.3 σ (after LEE) [1], while the CMS collaboration collected an integrated luminosity of 2.6 fb^{-1} and reports a significance 2.6 σ (local) that became 2.0 σ (after LEE) [2]. As tentative as the signal could be, it has motivated a large number of studies that attempt to reproduce its profile (for some works see for instance [3]).

Several ideas have been proposed to address the flavor problem [4]. For instance, textures and GUT-inspired relations, flavor symmetries and radiative generation, etc. The flavor symmetry approach can be supplemented with the Froggatt–Nielsen (FN) mechanism, which assumes that above some scale M_F there is a symmetry that forbids the appearance of Yukawa couplings; SM fermions are charged under this symmetry [which could be of Abelian type $U(1)_F$]. However, the Yukawa matrices can arise through non-renormalizable operators. The Higgs spectrum of these models could include light Higgs-flavons, which could mix with the scalar bosons. In these models, the diagonal flavor conserving (FC) couplings of the SM-like Higgs boson could deviate from the SM, while flavor violating (FV) couplings could be induced at small rates too, but still produce detectable signals. On the other hand, extending the Higgs sector of the SM opens up the possibility of including a scalar dark matter (DM) candidate, such as occurs with the well studied inert doublet model (IDM). There are important motivations to supplement this model with a complex singlet, for instance to have extra sources of CP violation, as in the IDM with a complex singlet (IDMS) recently studied [5].

In this paper we explore the possibility that the 750 GeV diphoton resonance [1,2], could be identified with a low-scale Higgs-flavon field H_F.[1] We work within a SM extension of the IDMS-type that contains two Higgs doublets and one complex FN singlet. The mixing of the doublet and the singlet induces FV couplings in the Higgs sector at the tree-level, which can induce the lepton flavor violating (LFV) Higgs decay $h \to \bar{\mu}\tau$ searched for at the LHC [6].

* Corresponding author.
E-mail address: gtv@fcfm.buap.mx (G. Tavares-Velasco).

[1] A different approach based on a flavor model has appeared recently [10].

http://dx.doi.org/10.1016/j.physletb.2016.08.029

2. The model

We consider a multi-Higgs model including one SM-like Higgs doublet Φ_s, an inert-type doublet Φ_n, and one FN scalar field (SM singlet S). The possibility of having light Higgs-flavon fields was studied in Ref. [7], and more recently in [8]. Besides breaking the electroweak symmetry, the Φ_s doublet gives masses to the quarks and leptons. By imposing a discrete symmetry, the Φ_n doublet will be of the inert-type and will contain a DM candidate [9].

In our model only the Z_2-even fields Φ_s and S_F acquire vacuum expectation values v and u, respectively. We will use the following field decomposition around the vacuum state:

$$\Phi_s = \begin{pmatrix} G^+ \\ \frac{1}{\sqrt{2}}\left(v+\phi^0+iG_z\right)\end{pmatrix}, \qquad \Phi_n = \begin{pmatrix} H^+ \\ \frac{1}{\sqrt{2}}\left(H+iA\right)\end{pmatrix}, \tag{1}$$

$$S_F = \frac{1}{\sqrt{2}}(u+s_1+ip_1). \tag{2}$$

The Higgs potential resembles that of the IDMS model studied in [5]. To reduce the free parameters, a $U(1)$ symmetry identified with the flavor symmetry is invoked. Its breaking helps out to address the hierarchy of the Yukawa couplings associated with the broad spectra of fermion masses. The scalar potential is invariant under CP and takes the form:

$$\begin{aligned} V = &-\frac{1}{2}\left[m_1^2\Phi_s^\dagger\Phi_s + m_2^2\Phi_n^\dagger\Phi_n\right] \\ &+\frac{1}{2}\left[\lambda_1\left(\Phi_s^\dagger\Phi_s\right)^2+\lambda_2\left(\Phi_n^\dagger\Phi_n\right)^2\right] \\ &+\lambda_3\left(\Phi_s^\dagger\Phi_s\right)\left(\Phi_n^\dagger\Phi_n\right)+\lambda_4\left(\Phi_s^\dagger\Phi_n\right)\left(\Phi_n^\dagger\Phi_s\right) \\ &+\frac{\lambda_5}{2}\left[\left(\Phi_s^\dagger\Phi_n\right)^2+\left(\Phi_n^\dagger\Phi_s\right)^2\right] \\ &-\frac{m_3^2}{2}S_F^*S_F-\frac{m_4^2}{2}(S_F^{*2}+S_F^2)+\lambda_{s1}(S_F^*S_F)^2 \\ &+\lambda_{ss}(\Phi_s^\dagger\Phi_s)(S_F^*S_F)+\lambda_{sn}(\Phi_n^\dagger\Phi_n)(S_F^*S_F). \end{aligned} \tag{3}$$

We are left with $U(1)$-symmetric terms (m_1^2, m_2^2, m_3^2, λ_{1-5}, λ_{s1}, λ_{ss}, and λ_{sn}) and a $U(1)$-soft-breaking term (m_4^2). An extensive analysis of the CP-violating version of this potential was presented in Ref. [5]. For the CP conserving case, imposing the minimization conditions for V results in the following relations:

$$m_1^2 = v^2\lambda_1 + u^2\lambda_{ss}, \tag{4}$$

$$m_3^2 = -2m_4^2 + 2u^2\lambda_{s1} + v^2\lambda_{ss}. \tag{5}$$

Since we are considering a CP-invariant potential, the CP-even (real) and CP-odd (imaginary) components of the mass matrix do not mix. Thus, the mass matrix for the real components in the basis (ϕ^0, H, s_1) is given by:

$$M_S^2 = \begin{pmatrix} \lambda_1 v & 0 & \lambda_{ss}uv \\ 0 & \frac{1}{2}(-m_3^2+\lambda^+v^2+\lambda_{sn}u^2) & 0 \\ \lambda_{ss}uv & 0 & 2\lambda_{s1}u^2 \end{pmatrix}, \tag{6}$$

where $\lambda^+ = \lambda_3+\lambda_4+\lambda_5$.

On the other hand, the mass matrix for imaginary components, in the basis (G_z, A, p_1), reads:

$$M_P^2 = \begin{pmatrix} 0 & 0 & 0 \\ 0 & \frac{1}{2}(-m_3^2+\lambda^-v^2+\lambda_{sn}u^2) & 0 \\ 0 & 0 & 2m_3^2 \end{pmatrix}, \tag{7}$$

where: $\lambda^- = \lambda_3+\lambda_4-\lambda_5$.

The neutral state $H(A)$ arising from the inert doublet does not mix with ϕ^0 nor s_1 (p_1), and the only massive charged state comes from the dark doublet, with $M_{H^+}^2 = \frac{1}{2}(-m_3^2+\lambda_3v^2+\lambda_{sn}u^2)$.

The real components of the Higgs (ϕ^0) and Higgs-flavon fields (s_1) do mix, and the mass eigenstates are obtained through the standard 2×2 rotation:

$$\begin{aligned} \phi^0 &= \cos\alpha h + \sin\alpha H_F, \\ s_1 &= -\sin\alpha h + \cos\alpha H_F. \end{aligned} \tag{8}$$

The mass eigenstates are h, which corresponds to the SM-like Higgs boson, with $m_h = 125$ GeV, whereas H_F and A_F are the heaviest states. The properties of H_F will depend on the properties of the SM Higgs boson due to the mixing. A_F does not couple to the gauge bosons, but it does to the SM fermions, including both FC and FV interactions.

In the forthcoming analysis of the Higgs decays we will use the trilinear vertex H_Fhh, which is given by:

$$\begin{aligned} g_{H_Fhh} = &\frac{1}{2}\Big[\lambda_{ss}(u\cos^3\alpha + v\sin^3\alpha) + 2u\sin^2\alpha\cos\alpha(3\lambda_{s1}-\lambda_{ss}) \\ &+ v\sin\alpha\cos^2\alpha(3\lambda_1 - 2\lambda_{ss})\Big] \simeq \frac{1}{2}\lambda_{ss}u \equiv \lambda u. \end{aligned} \tag{9}$$

The FN Lagrangian, which includes the terms that become Yukawa couplings after the $U(1)$ flavor symmetry is spontaneously broken, is given by:

$$\begin{aligned} \mathcal{L}_Y = &\rho_{ij}^u\left(\frac{S_F}{\Lambda_F}\right)^{n_{ij}}\bar{Q}_i d_j\tilde{\Phi} + \rho_{ij}^d\left(\frac{S_F}{\Lambda_F}\right)^{p_{ij}}\bar{Q}_i u_j\Phi \\ &+ \rho_{ij}^l\left(\frac{S_F}{\Lambda_F}\right)^{q_{ij}}\bar{L}_i l_j\Phi + \text{H.c.} \end{aligned} \tag{10}$$

where n_{ij}, p_{ij}, and q_{ij} denote the combination of Abelian charges for each fermion type. The Higgs-flavon field S_F is assumed to have flavor charge equal to -1, such that $\mathcal{L}_Y$ is $U(1)_F$-invariant. Then, the Yukawa couplings arise after the spontaneous breaking of the flavor symmetry, i.e. $\lambda_x \sim (\frac{<S_F>}{\Lambda_F})^{n_x}$, where $< S_F >$ denotes the Higgs-flavon vacuum expectation value, while Λ_F denotes the heavy mass scale, which represents the mass of heavy fields that transmit such symmetry breaking to the quarks and leptons. For specific structures of Yukawa matrices for each fermion type, see [9].

In the mass eigenstate basis we have the following Lagrangian for the Higgs-fermion couplings

$$\begin{aligned} \mathcal{L}_Y = &\frac{1}{v}[\bar{U}M_uU + \bar{D}M_dD + \bar{L}M_lL](c_\alpha h + s_\alpha H_F) \\ &+ \frac{v}{\sqrt{2}u}[\bar{U}_i\tilde{Z}^uU_j + \bar{D}_i\tilde{Z}^dD_j \\ &+ \bar{L}_i\tilde{Z}^lL_j](-s_\alpha h + c_\alpha H_F + iA_F). \end{aligned} \tag{11}$$

Here, the information about the size of FV Higgs couplings is contained in the $\tilde{Z}^f$ matrices. Thus, the (diagonal and non-diagonal) interactions of the scalar bosons (h, H_F, A_F) to the fermions f_i are:

$$\begin{aligned} (\bar{f}_i f_i h) &= \frac{c_\alpha}{v}\bar{M}_{ii}^f - \frac{s_\alpha v}{\sqrt{2}u}\tilde{Z}_{ii}^f \\ (\bar{f}_i f_j h) &= -\frac{s_\alpha v}{\sqrt{2}u}\tilde{Z}_{ij}^f \\ (\bar{f}_i f_i H_F) &= \frac{s_\alpha}{v}\bar{M}^f{}_{ii} + \frac{c_\alpha v}{\sqrt{2}u}\tilde{Z}_{ii}^f \\ (\bar{f}_i f_j H_F) &= \frac{c_\alpha v}{\sqrt{2}u}\tilde{Z}_{ij}^f \\ (\bar{f}_i f_j A_F) &= \frac{iv}{\sqrt{2}u}\tilde{Z}_{ij}^f\gamma^5 \end{aligned} \tag{12}$$

Table 1
Heavy quarks in the minimal FN mechanism.

Type	$SU(3)_c$	$SU(2)_L$	$U(1)_Y$	N_f
$P\ (\bar{P})$	3	2	$\frac{1}{6}$	3 (3)
$U\ (\bar{U})$	3	1	$\frac{2}{3}$	3 (3)
$D\ (\bar{D})$	3	1	-$\frac{1}{3}$	3 (3)

Besides the Yukawa couplings, we also need to specify the Higgs couplings to the vector bosons, which we write as $g_{h_i VV} = \chi_V^{h_i} g_{hVV}^{\rm SM}$, with the factor $\chi_V^{h_i}$ given as: $\chi_V^h = \cos\alpha$ and $\chi_V^{H_F} = \sin\alpha$. Moreover, since the Higgs couplings to the first generation fermions are highly suppressed, in order to study the FV Higgs couplings, which depends on the $\tilde{Z}^f$ matrices, we will consider a 2nd–3rd family sub-system. Namely, for up quarks the $\tilde{Z}^u$ matrix (in mass eigenstate basis), is given by:

$$\tilde{Z}^u = \begin{pmatrix} Y_{22}^u & Y_{23}^u \\ Y_{23}^u & 2s_u Y_{23}^u \end{pmatrix}, \qquad (13)$$

and similarly for down quarks and leptons. We find a relation among the parameters, such that we can express the $\rho_{ij}^{u,d}$ coefficients in terms of ratios of masses and the CKM angle $V_{cb} \simeq s_{23}$. Namely, we define: $r_u = m_c/m_t$, $r_d = m_s/m_b$, $r_1^u = Y_{22}^u/Y_{33}^u$, and $r_2^u = Y_{23}^u/Y_{33}^u$. Similarly $r_1^d = Y_{22}^d/Y_{33}^d$ and $r_2^d = Y_{23}^d/Y_{33}^d$. Within this approximation we have: $\tilde{Y}_{33}^f \simeq Y_{33}^f$ for $f = u, d$. Then, $r_1^f = r_f + r_2^f$, and the ratios of Yukawa couplings must satisfy the following relation:

$$r_2^u = r_2^d \frac{1 + r_d}{1 + r_u} - \frac{s_{23}}{1 + r_u}. \qquad (14)$$

Finally, it is worth mentioning that the FN mechanism can be ultraviolet (UV) completed via the introduction of heavy mirror fermions. The exact content depends on the specific model, as well as the desired Yukawa matrix. In general, one needs to introduce vector-like quarks, with the quantum numbers shown in Table 1. As will be discussed below, extra heavy vector-like quarks would be necessary to reproduce the signal for the 750 GeV resonance hinted at the LHC.

3. Scenarios for the Higgs-flavon couplings

We now turn to discuss the formula necessary to express all the relevant Higgs-flavon couplings, which will allow us to define some benchmark points:

1. FC Higgs couplings. Firstly, we will use LHC data to derive bounds on the Higgs-flavon couplings, following the analysis presented in Ref. [11]. The deviation from the SM Higgs couplings are assured to be small and are expressed as: $g_{hXX} = g_{hXX}^{sm}(1 + \epsilon_X)$. The results obtained in [11] give the following allowed ranges with 95% C.L.: $\epsilon_t = -0.21 \pm 0.23$, $\epsilon_b = -0.19 \pm 0.3$, and $\epsilon_\tau = 0 \pm 0.18$; while for the W and Z gauge bosons it is found $\epsilon_W = -0.15 \pm 0.14$ and $\epsilon_Z = -0.01 \pm 0.13$.

We will use the strongest constraints, which come from a combination of ϵ_Z and ϵ_t, in such a way that the resulting constraint on the mixing angle is $0.86 < \cos\alpha < 1.0$.

2. FV Higgs couplings to up-type quarks. As far as the couplings with up-type quarks are concerned, we will follow the method outlined in Ref. [9]. Namely, we will consider the following sample values: $r_d^2 = 0.05, 0.1$, and 0.3. Table 2 shows the values of the entries for the up-type quark $\tilde{Z}^u$ matrix in the 2nd–3rd family scenario. We choose to focus on the up-quark sector because we want to obtain an estimate for the most relevant predictions of the model.

Table 2
Relevant elements of the matrix $\tilde{Z}_{ij}^u$ for up-type quarks.

Scenario	$\tilde{Z}_{33}^u$	$\tilde{Z}_{23}^u$	$\tilde{Z}_{22}^u$
X1	4×10^{-4}	2×10^{-2}	2×10^{-4}
X2	1.4×10^{-2}	1.2×10^{-1}	7.2×10^{-3}
X3	0.27	0.52	0.14

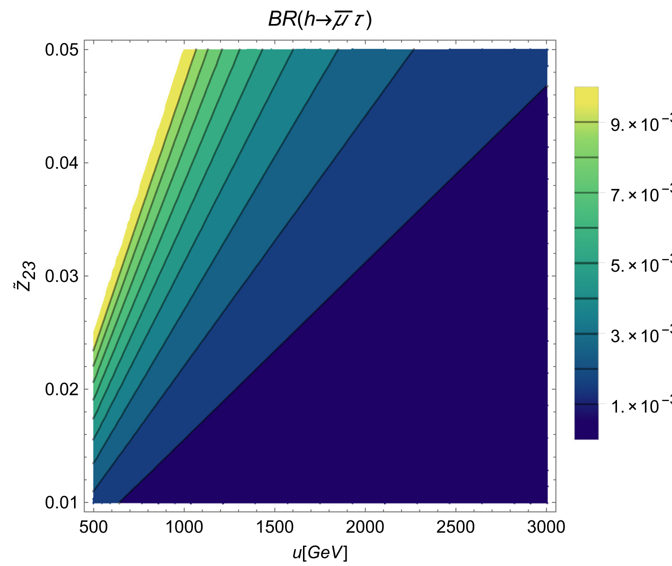

Fig. 1. Contour plot for the branching ratio of the flavor violating decay of the SM Higgs boson $h \to \bar{\mu}\tau$ in the $u - \tilde{Z}_{23}$ plane. For the parameter values we use $s_\alpha = 0.4$ and $\tilde{Z}_{33} = 0.15$.

3. LFV Higgs couplings. These couplings are written in terms of the parameters ρ_{ij}, which appear in the charged lepton mass matrix, and are of the order of $O(1)$. Namely,

$$\tilde{Z}_{33}^l = 2\sqrt{2}\frac{m_\tau}{v} \simeq 1.95 \times 10^{-2},$$
$$\tilde{Z}_{23}^l = 4\lambda^4 \rho_{23}^l \simeq 10^{-2}\rho_{23}^l,$$
$$\tilde{Z}_{22}^l = 4.1 \times 10^{-2}\rho_{23}^l + 2.41 \times 10^{-3}. \qquad (15)$$

We will consider values of $\rho_{23}^l = 0.25, 0.75$.

An interesting probe of FV Higgs couplings is provided by the decay $h \to \bar{\mu}\tau$, which was initially studied in Refs. [12,13]. Subsequent studies on the detectability of the signal appeared soon after [14–16]. Precise loop calculations with massive neutrinos, SUSY and other models were worked out in [17–20]. A search for this decay at the LHC Run I [21] observed a slight excess of signal events with a significance of 2.4 standard deviations. Several works appeared trying to explain that result [22]. However a recent report [23] rules out any excess and sets the limit $BR(h \to \bar{\mu}\tau) < 1.2 \times 10^{-2}$ with 95% C.L. Such a bound is very loose and irrespectively of the dismissal of the excess, the search for LFV Higgs decays represents a great opportunity to find new physics at the LHC Run II. We show in Fig. 1 the contour plot for the branching ratio of the SM Higgs boson decay $h \to \bar{\mu}\tau$ in the $u - \tilde{Z}_{23}$ plane, with $s_\alpha = 0.4$ and $\tilde{Z}_{33} = 0.15$. We observe that values as large as 10^{-2} can be reached for u around 500 GeV and $\tilde{Z}_{23} = 0.02$. An improvement of the experimental limit on the $h \to \bar{\mu}\tau$ would put strong constraints on the parameter values.

4. Higgs-flavon decay modes

The calculation of the two-body tree-level decays is straightforward and so is that of the two-body one-loop decays. To illustrate

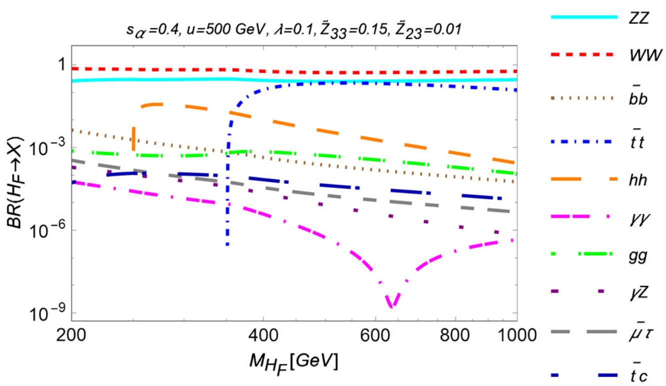

Fig. 2. Branching ratios for the relevant decays of the Higgs-flavon state H_F as functions of M_{H_F} for the indicated set of parameter values.

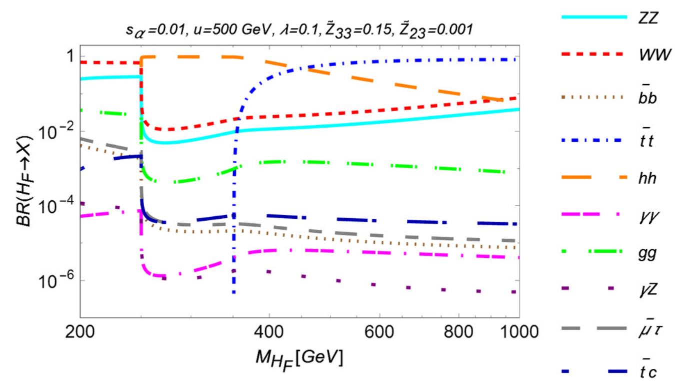

Fig. 3. Branching ratios for the relevant decays of the Higgs-flavon state H_F as functions of M_{H_F} for the indicated set of parameter values.

the behavior of the Higgs-flavon decays we will consider two scenarios of interest, namely, a middle and a tiny value of the mixing angle s_α. We first consider the following set of parameter values: $s_\alpha = 0.4$, $u = 500$ GeV, $\lambda = 0.1$, $\tilde{Z}_{33} = 0.15$, and $\tilde{Z}_{23} = 0.01$. The relevant branching ratios of the Higgs-flavon decays, as functions of the Higgs-flavon mass M_{H_F}, are shown in Fig. 2. We observe that in this scenario the decay modes $H_F \to WW$, and $H_F \to ZZ$ are the dominant ones, with branching ratios of the order of 0.7 and 0.35, respectively. These decay channels remain the dominant ones even after the threshold of the $H_F \to t\bar{t}$ decay, which in turn can reach a branching ratio of around 0.2 at most. We also notice that the decay $H \to hh$ could reach a branching ratio of the order of ten percent approximately, although such a value is highly dependent on the value of the λ parameter. Such a branching ratio would open up the possibility for the search of this decay mode at LHC13. As far as the one-loop induced decays are concerned, they are very suppressed. In particular, the branching ratio of the $H_F \to \gamma\gamma$ decay shows a large dip around 600 GeV, where it is negligible. For the parameter values used, the flavor changing decays $H_F \to \bar{\mu}\tau$ and $H_F \to \bar{c}t$ can reach branching ratios of the order of 10^{-3}–10^{-4} for a Higgs-flavon with intermediate mass.

We now turn to analyze the scenario with very small s_α, namely, we take $s_\alpha = 0.01$ and use the same values as above for all the remaining parameters. The branching ratios for the decays of the Higgs-flavon change are shown in Fig. 3 as functions of the Higgs-flavon mass. As expected due to the dependence of the Higgs-flavon couplings on s_α, there is a notorious change in the behavior of the decay widths. For an intermediate mass, the dominant decay channels are still those into a gauge boson pair, but the $H_F \to hh$ decay becomes the dominant one after it is open and until the threshold of the $H_F \to \bar{t}t$ decay is reached. For a heavier Higgs-flavon, the $H_F \to \bar{t}t$ becomes dominant, which is due to the extra term proportional to c_α appearing in the associated coupling constant. The one-loop induced decays have an enhanced branching fraction, but the $H_F \to \gamma\gamma$ and $H_F \to Z\gamma$ channels are still very suppressed. For a lower value of s_α the $H_F \to WW$ and $H_F \to ZZ$ decay widths, though nonvanishing, will become considerably suppressed, which means that the $H_F \to gg$ and $H_F \to \bar{t}t$ channels would become the dominant ones, with the decay $H_F \to \gamma\gamma$ having an enhanced branching ratio. All other Higgs-flavon decays to light fermions would have a negligibly branching ratio. We will analyze below the scenario in which extra vector-like fermions from the UV completion of the Higgs-flavon model contribute at the one-loop level to the $H_F \to gg$ and $H_F \to \gamma\gamma$ decays. This could result in a significant change in the behavior of the Higgs-flavon decays.

It is worth analyzing more detailed the $H_F \to hh$ decay. Fig. 4 shows that in the region of the parameter space enclosed by

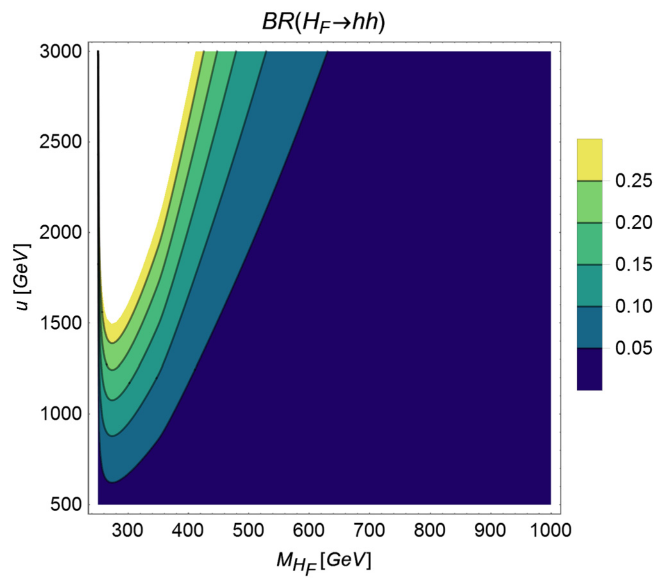

Fig. 4. Contour plot for the $H_F \to hh$ branching ratio in the $u - M_{H_F}$ plane. For the parameter values we use $s_\alpha = 0.4$, $\lambda = 0.1$, $\tilde{Z}_{33} = 0.15$ and $\tilde{Z}_{23} = 0.01$.

500 GeV $< u <$ 3000 GeV and 250 GeV $< M_{H_F} <$ 1000 GeV, the branching fraction $BR(H_F \to hh)$ can be of the order of about 0.01, which seems amenable to be searched for at the LHC13.

5. The Higgs-flavon as the 750 GeV diphoton resonance

Besides extending the limits on new physics scale, the ATLAS and CMS collaborations have reported preliminary evidences for a new resonance at 750 GeV in the two-photon channel, which could come from either a new spin-0 or spin-2 particle. We will explore the possibility that such a resonance could be identified with the Higgs-flavon field H_F. By studying the decays of this Higgs-flavon, we can identify the regions of the parameter space that would accommodate the new 750 GeV signal. A summary of the profile of diphoton resonance at 750 GeV, shows the following:

1. ATLAS excess of about 14 events (with selection efficiency 0.4) appears in at least two energy bins, suggesting a width of about 45 GeV (i.e. $\Gamma/M \simeq 0.06$). The best CMS fit has a narrow width, while assuming a large width ($\Gamma/M \simeq 0.06$) decreases the significance, which corresponds to a cross section of about 6 fb.

2. The anomalous events are not accompanied by significant missing energy, nor leptons or jets. No resonances at invariant mass 750 GeV are seen in the new data in ZZ, W^+W^-, or

jj events, and no $\gamma\gamma$ resonances were seen in Run 1 data at $\sqrt{s}=8$ TeV, although both CMS and ATLAS data showed a mild upward fluctuation at $m_{\gamma\gamma}=750$ GeV. The data at $\sqrt{s}=8$ TeV and 13 TeV are compatible at 2 σ if the signal cross section grows by at least a factor of 5.

3. For a spin-0 resonance produced from gluon fusion and decaying mainly into two photons, the signal rate is reproduced for

$$R_\Gamma^g=\frac{\Gamma_{\gamma\gamma}\Gamma_{gg}}{MM}\simeq 1.1\times 10^{-6}\frac{\Gamma}{M}\simeq 6\times 10^{-8}, \qquad (16)$$

with M the scalar boson mass.

4. When the resonance S is produced from bottom quark annihilation, the signal is reproduced for

$$R_\Gamma^b=\frac{\Gamma_{\gamma\gamma}\Gamma_{bb}}{MM}\simeq 1.9\times 10^{-4}\frac{\Gamma}{M}\simeq 1.1\times 10^{-5}. \qquad (17)$$

5. The combined data from ATLAS and CMS at $\sqrt{s}=8$ and $\sqrt{s}=13$ TeV result in the following production cross section for the diphoton channel

$$\sigma(pp\to S\to\gamma\gamma)=6.6\pm 1.3\text{ fb}. \qquad (18)$$

At the LHC the Higgs-flavon would be mainly produced via gluon fusion mediated by the triangle diagram carrying SM quarks, as shown in Fig. 5. The dominant contribution would arise from the top quark. We will consider that there are also contributions coming from the heavy vector-like quarks predicted by the UV completion of the Higgs-flavon model. Apart from reproducing the experimental data for the diphoton decay width at $\sqrt{s}=13$ TeV, the Higgs-flavon also must satisfy the experimental bounds set by the ATLAS and CMS collaborations (see Table 3) on the $\sqrt{s}=8$ TeV cross section for the production of a scalar resonance decaying into gauge boson pairs, gluon pairs, etc. We will thus examine whether there is a region of the parameter space of the Higgs-flavon model that is in accordance with experimental data. A quick glance at Figs. 2 and 3 allows us to conclude that the following conditions are to be fulfilled: a very small s_α to achieve small $H_F\to WW$ and $H_F\to ZZ$ branching ratios, negligible FV couplings in order to suppress the tree-level decays $H_F\to\bar{\mu}\tau$ and $H_F\to\bar{c}t$, and an increase of the Higgs-flavon diphoton production. The latter can only be achieved through an enhancement of the $H_F\to\gamma\gamma$ decay width along with an increase of the gluon fusion production mode, which requires the introduction of additional loop contributions from charged/colored particles. Since the contribution of a singly charged scalar is rather suppressed, an enhancement of the $H_F\to\gamma\gamma$ decay can be achieved with the addition of extra vector-like fermions, which can also enhance the $H_F\to gg$ partial width, so a $pp\to H_F\to\gamma\gamma$ cross section of the order of 1–10 fb can be reached at $\sqrt{s}=13$ TeV. Vector-like fermions are required to not to spoil the constraints on electroweak precision data. Within the context of our model these heavy quanta could be naturally identified with the heavy vector-like fermions that would arise from the UV completion of the FN mechanism.

A detailed discussion of the FN UV completion is beyond the purpose of this letter and we refrain the interested reader to [33] and References therein. No matter the details of the specific vector-like fermion model, for the purpose of our analysis is enough to consider an scenario with N degenerate vector-like quarks with the following effective interaction to the Higgs-flavon

$$\mathcal{L}=i\frac{C_Q m_Q}{v}\bar{Q}\,Q\,H_F, \qquad (19)$$

where C_Q stand for the coupling constant that can be known once a specific model is considered. There are models that also predict vector-like leptons but they do not yield the necessary enhancement to the $pp\to H_F\to\gamma\gamma$ cross section to reproduce the observed signal and will not be considered here. As for the couplings of the vector-like quarks to the SM gauge bosons, they can be written as:

$$\mathcal{L}=eq_Q\,\bar{Q}\,\gamma^\mu Q\,A_\mu+g_s\bar{Q}\,\gamma^\mu Q\,G_\mu+\frac{g}{c_W}\bar{Q}\,\gamma^\mu(T_3-s_W^2\,Q)Q\,Z_\mu. \qquad (20)$$

So, the calculation of the fermion loop of Fig. 5 proceeds as usual. The result for the two-photon decay width, including contributions of charged fermions and the W gauge boson can be written as

$$\Gamma(H_F\to\gamma\gamma)=\frac{\alpha^2 m_{H_F}^3}{1024\pi^3 m_W^2}\left|\sum_{s=f,W^\pm}A_s^{H_F\gamma\gamma}(\tau_s)\right|^2, \qquad (21)$$

where $\tau_s=4m_s^2/m_{H_F}^2$ and

$$A_s^{H_F\gamma\gamma}(x)=\begin{cases}-\sum_f\frac{2m_W g_{H_F\bar{f}f}N_c Q_f^2}{m_f}\left[2x(1+(1-x)f(x))\right] & s=f,\\ \frac{g_{H_FWW}}{m_W}\left[2+3x+3x(2-x)f(x)\right] & s=W,\end{cases} \qquad (22)$$

with $g_{H_F\bar{f}f}$ and g_{H_FWW} the respective coupling constants and

$$f(x)=\begin{cases}\left[\arcsin\left(\frac{1}{\sqrt{x}}\right)\right]^2 & x\geq 1,\\ -\frac{1}{4}\left[\log\left(\frac{1+\sqrt{1-x}}{1-\sqrt{1-x}}\right)-i\pi\right]^2 & x<1.\end{cases} \qquad (23)$$

The contributions of a singly charged scalar boson is subdominant and can be neglected. For a heavy Higgs-flavon, the main contribution arises from the heaviest charged fermion. As for the $H_F\to gg$ decay, the respective decay width can be obtained from (21) by taking the quark contribution only and making the replacements $\alpha\to\alpha_s$ and $NQ_f^2\to\sqrt{2}$ [34]. Next-to-leading order contributions

Table 3
Experimental upper limits imposed by the CMS and ATLAS collaborations on the $pp\to S\to X$ cross section at $\sqrt{s}=8$ TeV with 95 % C.L. for a scalar resonance S with a mass of 750 GeV.

X	CMS bound [fb]	ATLAS bound [fb]
WW	220 [24]	38 [25]
ZZ	27 [24]	12 [26]
$\bar{t}t$	600 [27]	700 [28]
hh	52 [29]	35 [30]
gg	1800 [31]	–
$Z\gamma$	–	6 [32]
$\gamma\gamma$	1.3 [2]	10 [1]

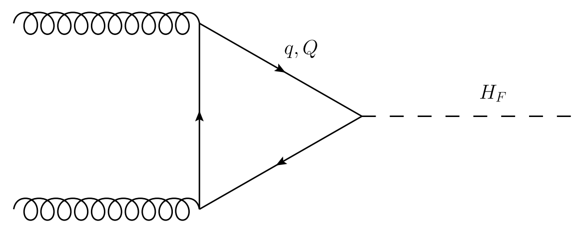

Fig. 5. Feynman diagram for the leading order contribution to Higgs-flavon production via gluon fusion. In the loop can circulate a SM quark (q) or a new vector like quark (Q) of the UV completion of the Higgs-flavon model. A similar diagram induces the $H_F\to\gamma\gamma$ decay except that we need to include contributions from all other electrically charged particles.

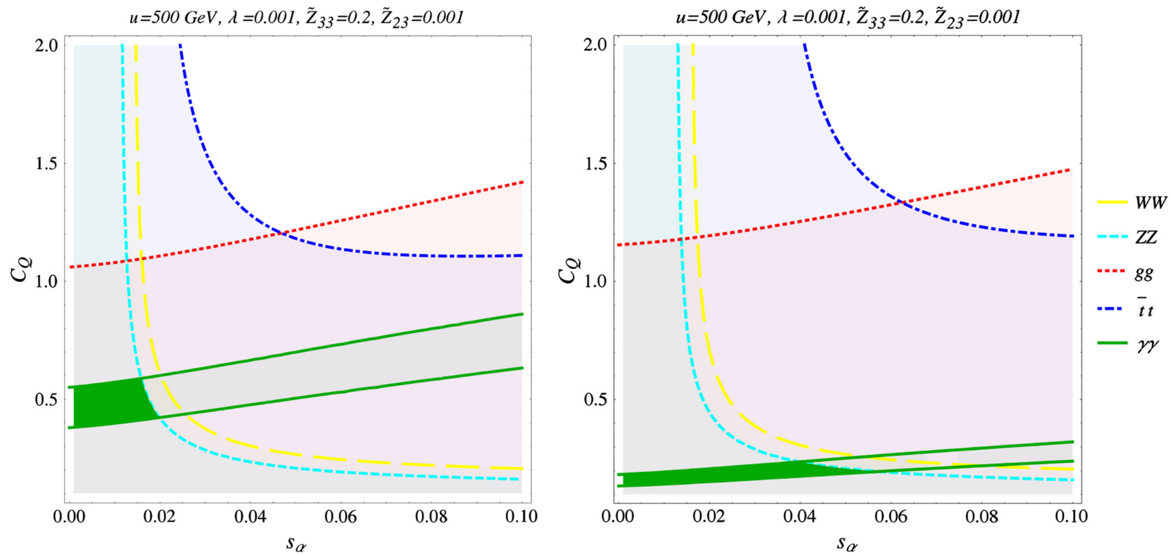

Fig. 6. Area allowed in the C_Q vs s_α plane by the LHC constraints on the $\sqrt{s} = 8$ TeV $pp \to H_F \to X$ production cross section mediated by a 750 GeV Higgs-flavon for the indicated set of parameter values. We consider the addition of 3 vector-like quarks with mass $m_Q = 1000$ GeV and charge 2/3 (left plot) and 5/3 (right plot). The area below each curve is the one allowed by the particular production mode at $\sqrt{s} = 8$ TeV (see Table 3) and the dark area represents the region where the $\sqrt{s} = 13$ TeV $pp \to H_F \to \gamma\gamma$ cross section lies between 6.6 ± 1.3 fb.

have also been calculated and the results are summarized for instance in Ref. [34]. The production cross section of a scalar resonance decaying into the X channel is given by

$$\sigma(pp \to H_F \to X) = \sigma(pp \to H_F)_{GF} BR(H_F \to X), \tag{24}$$

where $\sigma(pp \to H_F)_{GF}$ is the cross section for the production of a scalar resonance via gluon fusion at the LHC [34].

We will now consider a scenario with 3 degenerate vector-like charge 2/3 quarks Q (they can be introduced in the model as $SU(2)$ singlets as shown in Table 1) and find the region in the C_Q vs s_α plane consistent with the LHC Run I bounds on the production cross section of a scalar resonance decaying into a final state X, as shown in Table 3, for the following set of parameter values: $u = 500$ GeV, $\tilde{Z}_{33} = 0.2$, $\lambda = 0.001$, and $\tilde{Z}_{23} = 0.001$. It means that we are assuming that the $H_F \to hh$, $H_F \to \bar{\mu}\tau$, and $H_F \to \bar{c}t$ decay channels have a negligible decay width. For the mass of the vector-like quarks we use $m_Q = 1000$ GeV to fulfill the current experimental bounds. The results are shown in the left plot of Fig. 6, where the area below each curve is consistent with the LHC Run I data for the production cross section $\sigma(pp \to H_F \to X)$ and the dark area is the one in which the diphoton cross section $\sigma(pp \to H_F \to \gamma\gamma)$ lies between 6.3 ± 1.3 fb, thereby reproducing the observed diphoton anomaly. It is important to notice that we choose to use the strongest constraints of Table 3. To estimate the production cross section we implemented a code with the formulas for the decay widths of a scalar Higgs boson as well as the gluon fusion cross section [34] and used the CT10 gluon parton distributions [35]. We note that the experimental data on the ZZ and gg final states provides strong constraints on the Higgs-flavon couplings but there is a surviving tiny area in which the Higgs-flavon model can reproduce the experimental data on the diphoton resonance while still being consistent with the experimental constraints on the $pp \to S \to X$ production cross section. For (s_α, C_Q) values lying inside the allowed area, the dominant decay modes are $H_F \to gg$ and $H_F \to \bar{t}t$. If a larger number of vector-like charge 2/3 quarks are considered, the allowed area will shift downwards and lower C_Q values will be allowed. While a large number of vector-like charge $-1/3$ quarks would be required to reproduce the diphoton signal, there is also the possibility of vector-like quarks of exotic charge. We consider an scenario with 3 vector-like charge 5/3 quarks, which can be introduced in a hypercharge 7/6 $SU(2)$ doublet and will be accompanied by a vector-like charge 2/3 quark. We take $m_Q = 1000$ GeV and show the resulting constraints in the right plot of Fig. 6. In this scenario the allowed region not only has shifted downwards but also has shrunk considerably. It is worth mentioning that the experimental limits on the $\bar{b}b$, hh and $Z\gamma$ final states provide no useful constraints. Also the Higgs-flavon decays into light quarks $H_F \to \bar{q}q$ pose no problem to satisfy the LHC dijet constraints as the corresponding coupling constants are proportional to s_α and thus yield a negligible decay rate for very small s_α. Furthermore, these vector-like quarks would not produce dangerous effects on the loop induced SM Higgs couplings if there is a small mixing of the Higgs-flavon with the SM Higgs boson.

We now fix the mixing angle s_α to the tiny value 0.001 and find the allowed region in the C_Q vs $\tilde{Z}_{33}$ plane. The results are shown in the left and right plots of Fig. 7 for the parameter values of the scenarios of Fig. 6. In this case the diboson channels $H_F \to WW$ and $H_F \to ZZ$ are considerably suppressed and the gg and $\bar{t}t$ final states are the only ones that provide useful constraints. Furthermore, in this scenario the Higgs-flavon decay width is completely dominated by the $H_F \to gg$ and $H_F \to \bar{t}t$ decay widths.

For typical values of parameter values lying inside the allowed area the total decay width of the Higgs-flavon is of order a few GeV at most. This seems to be in contradiction with the ATLAS data, which point to a large decay width of about 45 GeV. However, the CMS data hint to a narrow resonance with a decay width of a few GeVs. It is expected that these estimates change considerably once more data are available, provided that the diphoton resonance is confirmed. In such a case, a more detailed analysis of the scenario posed by the Higgs-flavon model would be in order.

6. Conclusions and outlook

In this work, we have studied a model including one Higgs doublet that participates in the spontaneous symmetry breaking and an extra inert doublet, which contains a DM candidate, together with a FN scalar field. We have found that this model allows for an interesting phenomenology to be searched for at the LHC. For instance, mixing of the Higgs doublets with a Higgs-flavon field H_F

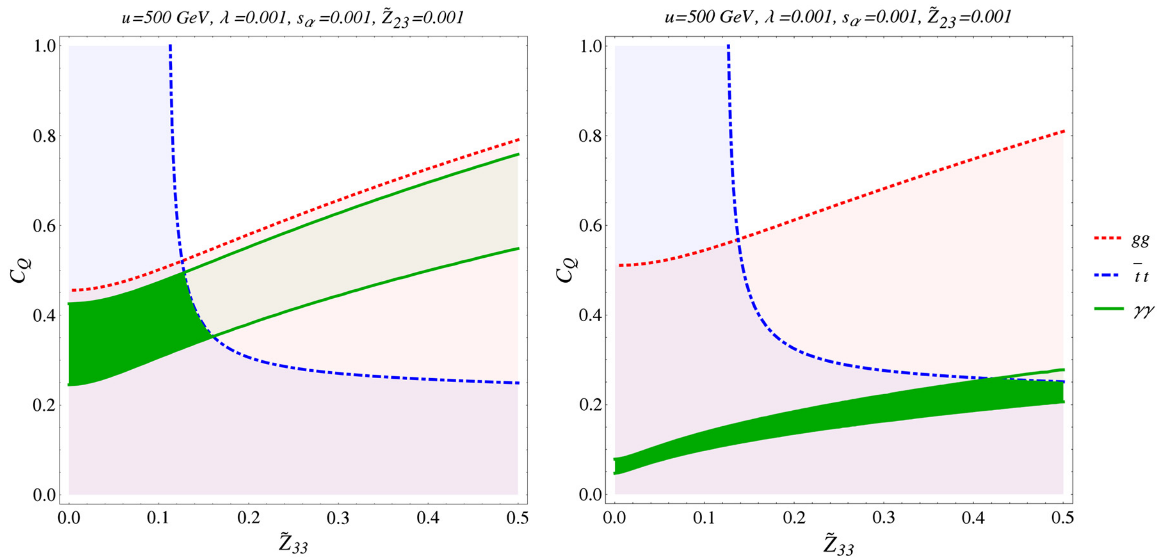

Fig. 7. The same as in Fig. 6, but for the area allowed in the C_Q vs $\tilde{Z}_{33}$ plane.

is included, which generates the Yukawa hierarchies and might induce flavor violating Higgs couplings at non-negligible rates. Constraints on these couplings, derived from the Higgs searches at the LHC, and their implications for scalar anomalies were studied. It was found that this model allows for a region of the parameter space where a branching ratio of the SM Higgs decay $h \to \bar{\mu}\tau$ can be at the level of the current experimental bound. We examined the possibility that the scalar Higgs-flavon H_F could be identified with the 750 GeV scalar resonance preliminarily observed at the LHC13 in the two-photon final state, and found the allowed area of the parameter space consistent with the ATLAS and CMS constraints on the rate of the $\sqrt{s} = 8$ TeV $pp \to S \to X$ production cross section for a 750 GeV scalar resonance decaying into weak gauge bosons, gluons, and top quark pairs. In order to reproduce the diphoton signal, the parameter space of the model must be tightly constrained, though a tiny area consistent with the experimental data still would survive. Furthermore, in this scenario the total decay width of the Higgs-flavon would be of the order of a few GeVs, as preferred by the CMS data, and decays channels such as $H_F \to hh$ and $H_F \to \bar{\mu}\tau$ would be highly suppressed, with branching ratios below the 10^{-6} level. Another possibility is that a pseudoscalar Higgs-flavon A_F predicted by the model could be identified with the 750 GeV resonance, but the analysis and conclusions would be rather similar. A definitive conclusion could be drawn once more data are available. We also examined another scenario in which the Higgs-flavon is not necessarily identified with the 750 GeV resonance. In this case there is an area of the parameter space in which it is feasible that the decay $H_F \to hh$ could have a significant branching ratio, which would open up the possibility for its study at the LHC. A more lengthy and detailed study of the phenomenology of this model will be published elsewhere.

Acknowledgements

Support from CONACYT-SNI (Mexico) and VIEP (BUAP) are acknowledged.

References

[1] Search for resonances decaying to photon pairs in 3.2 fb^{-1} of pp collisions at $s = 13$ TeV with the ATLAS detector, Technical report ATLAS-CONF-2015-081, CERN, Geneva, 2015, http://cds.cern.ch/record/2114853.

[2] CMS Collaboration, Search for new physics in high mass diphoton events in proton–proton collisions at $s = 13$ TeV, CMS-PAS-EXO-15-004, https://cds.cern.ch/record/2114808, 2015.

[3] S. Di Chiara, L. Marzola, M. Raidal, Phys. Rev. D 93 (9) (2016) 095018, http://dx.doi.org/10.1103/PhysRevD.93.095018, arXiv:1512.04939 [hep-ph];
R. Franceschini, et al., J. High Energy Phys. 1603 (2016) 144, http://dx.doi.org/10.1007/JHEP03(2016)144, arXiv:1512.04933 [hep-ph];
J. Ellis, S.A.R. Ellis, J. Quevillon, V. Sanz, T. You, J. High Energy Phys. 1603 (2016) 176, http://dx.doi.org/10.1007/JHEP03(2016)176, arXiv:1512.05327 [hep-ph];
K. Harigaya, Y. Nomura, Phys. Lett. B 754 (2016) 151, http://dx.doi.org/10.1016/j.physletb.2016.01.026, arXiv:1512.04850 [hep-ph];
D. Buttazzo, A. Greljo, D. Marzocca, Eur. Phys. J. C 76 (3) (2016) 116, http://dx.doi.org/10.1140/epjc/s10052-016-3970-7, arXiv:1512.04929 [hep-ph];
A. Falkowski, O. Slone, T. Volansky, J. High Energy Phys. 1602 (2016) 152, http://dx.doi.org/10.1007/JHEP02(2016)152, arXiv:1512.05777 [hep-ph];
R.S. Gupta, S. Jäger, Y. Kats, G. Perez, E. Stamou, arXiv:1512.05332 [hep-ph];
M. Low, A. Tesi, L.T. Wang, J. High Energy Phys. 1603 (2016) 108, http://dx.doi.org/10.1007/JHEP03(2016)108, arXiv:1512.05328 [hep-ph];
S.D. McDermott, P. Meade, H. Ramani, Phys. Lett. B 755 (2016) 353, http://dx.doi.org/10.1016/j.physletb.2016.02.033, arXiv:1512.05326 [hep-ph];
A. Pilaftsis, Phys. Rev. D 93 (1) (2016) 015017, http://dx.doi.org/10.1103/PhysRevD.93.015017, arXiv:1512.04931 [hep-ph];
A. Kobakhidze, F. Wang, L. Wu, J.M. Yang, M. Zhang, Phys. Lett. B 757 (2016) 92, http://dx.doi.org/10.1016/j.physletb.2016.03.067, arXiv:1512.05585 [hep-ph];
B. Dutta, Y. Gao, T. Ghosh, I. Gogoladze, T. Li, Phys. Rev. D 93 (5) (2016) 055032, http://dx.doi.org/10.1103/PhysRevD.93.055032, arXiv:1512.05439 [hep-ph];
K. Ghorbani, H. Ghorbani, arXiv:1601.00602 [hep-ph];
M.T. Frandsen, I.M. Shoemaker, arXiv:1603.09354 [hep-ph];
X.F. Han, L. Wang, Phys. Rev. D 93 (5) (2016) 055027, http://dx.doi.org/10.1103/PhysRevD.93.055027, arXiv:1512.06587 [hep-ph];
X.F. Han, L. Wang, J.M. Yang, arXiv:1601.04954 [hep-ph];
A. Angelescu, A. Djouadi, G. Moreau, Phys. Lett. B 756 (2016) 126, http://dx.doi.org/10.1016/j.physletb.2016.02.064, arXiv:1512.04921 [hep-ph];
P.S.B. Dev, R.N. Mohapatra, Y. Zhang, J. High Energy Phys. 1602 (2016) 186, http://dx.doi.org/10.1007/JHEP02(2016)186, arXiv:1512.08507 [hep-ph].

[4] G. Isidori, Y. Nir, G. Perez, Annu. Rev. Nucl. Part. Sci. 60 (2010) 355, arXiv:1002.0900 [hep-ph].

[5] C. Bonilla, D. Sokolowska, J.L. Diaz-Cruz, M. Krawczyk, N. Darvishi, arXiv:1412.8730 [hep-ph].

[6] K. Huitu, V. Keus, N. Koivunen, O. Lebedev, arXiv:1603.06614 [hep-ph].

[7] I. Dorsner, S.M. Barr, Phys. Rev. D 65 (2002) 095004, arXiv:hep-ph/0201207.

[8] K. Tsumura, L. Velasco-Sevilla, Phys. Rev. D 81 (2010) 036012, arXiv:0911.2149 [hep-ph];
E.L. Berger, S.B. Giddings, H. Wang, H. Zhang, Phys. Rev. D 90 (7) (2014) 076004, arXiv:1406.6054 [hep-ph];
L. Calibbi, Z. Lalak, S. Pokorski, R. Ziegler, J. High Energy Phys. 1207 (2012) 004, http://dx.doi.org/10.1007/JHEP07(2012)004, arXiv:1204.1275 [hep-ph];
L. Calibbi, A. Crivellin, B. Zaldívar, Phys. Rev. D 92 (1) (2015) 016004, http://dx.doi.org/10.1103/PhysRevD.92.016004, arXiv:1501.07268 [hep-ph];
I. Medeiros Varzielas, O. Fischer, J. High Energy Phys. 1601 (2016) 160, http://dx.doi.org/10.1007/JHEP01(2016)160, arXiv:1512.00869 [hep-ph];

I. de Medeiros Varzielas, O. Fischer, V. Maurer, J. High Energy Phys. 1508 (2015) 080, http://dx.doi.org/10.1007/JHEP08(2015)080, arXiv:1504.03955 [hep-ph].
[9] J.L. Diaz-Cruz, arXiv:1405.0990 [hep-ph].
[10] C. Bonilla, M. Nebot, R. Srivastava, J.W.F. Valle, arXiv:1602.08092 [hep-ph].
[11] P.P. Giardino, K. Kannike, I. Masina, M. Raidal, A. Strumia, arXiv:1303.3570 [hep-ph].
[12] A. Pilaftsis, Phys. Lett. B 285 (1992) 68.
[13] J.L. Diaz-Cruz, J.J. Toscano, Phys. Rev. D 62 (2000) 116005, arXiv:hep-ph/9910233.
[14] T. Han, D. Marfatia, Phys. Rev. Lett. 86 (2001) 1442, arXiv:hep-ph/0008141.
[15] K.A. Assamagan, A. Deandrea, P.A. Delsart, Phys. Rev. D 67 (2003) 035001, arXiv:hep-ph/0207302.
[16] S. Kanemura, T. Ota, K. Tsumura, Phys. Rev. D 73 (2006) 016006, arXiv:hep-ph/0505191.
[17] J.L. Diaz-Cruz, J. High Energy Phys. 0305 (2003) 036, arXiv:hep-ph/0207030.
[18] E. Arganda, A.M. Curiel, M.J. Herrero, D. Temes, Phys. Rev. D 71 (2005) 035011, arXiv:hep-ph/0407302.
[19] A. Brignole, A. Rossi, Nucl. Phys. B 701 (2004) 3, arXiv:hep-ph/0404211.
[20] J.L. Diaz-Cruz, D.K. Ghosh, S. Moretti, Phys. Lett. B 679 (2009) 376, arXiv:0809.5158 [hep-ph].
[21] V. Khachatryan, et al., CMS Collaboration, arXiv:1502.07400 [hep-ex].
[22] For a recent review see A. Vicente, arXiv:1503.08622 [hep-ph].
[23] CMS Collaboration, CMS-PAS-HIG-16-005.
[24] V. Khachatryan, et al., CMS Collaboration, J. High Energy Phys. 1510 (2015) 144, http://dx.doi.org/10.1007/JHEP10(2015)144, arXiv:1504.00936 [hep-ex].
[25] G. Aad, et al., ATLAS Collaboration, J. High Energy Phys. 1601 (2016) 032, http://dx.doi.org/10.1007/JHEP01(2016)032, arXiv:1509.00389 [hep-ex].
[26] G. Aad, et al., ATLAS Collaboration, Eur. Phys. J. C 76 (1) (2016) 45, http://dx.doi.org/10.1140/epjc/s10052-015-3820-z, arXiv:1507.05930 [hep-ex].
[27] CMS Collaboration, CMS-PAS-B2G-12-006.
[28] G. Aad, et al., ATLAS Collaboration, J. High Energy Phys. 1508 (2015) 148, http://dx.doi.org/10.1007/JHEP08(2015)148, arXiv:1505.07018 [hep-ex].
[29] V. Khachatryan, et al., CMS Collaboration, Phys. Lett. B 749 (2015) 560, http://dx.doi.org/10.1016/j.physletb.2015.08.047, arXiv:1503.04114 [hep-ex].
[30] G. Aad, et al., ATLAS Collaboration, Phys. Rev. D 92 (2015) 092004, http://dx.doi.org/10.1103/PhysRevD.92.092004, arXiv:1509.04670 [hep-ex].
[31] V. Khachatryan, et al., CMS Collaboration, arXiv:1604.08907 [hep-ex].
[32] G. Aad, et al., ATLAS Collaboration, Phys. Lett. B 738 (2014) 428, http://dx.doi.org/10.1016/j.physletb.2014.10.002, arXiv:1407.8150 [hep-ex].
[33] S.A.R. Ellis, R.M. Godbole, S. Gopalakrishna, J.D. Wells, J. High Energy Phys. 1409 (2014) 130, http://dx.doi.org/10.1007/JHEP09(2014)130, arXiv:1404.4398 [hep-ph].
[34] A. Djouadi, Phys. Rep. 457 (2008) 1, http://dx.doi.org/10.1016/j.physrep.2007.10.004, arXiv:hep-ph/0503172.
[35] S. Dulat, et al., Phys. Rev. D 89 (11) (2014) 113002, http://dx.doi.org/10.1103/PhysRevD.89.113002, arXiv:1310.7601 [hep-ph].